Available online at www.sciencedirect.com
SCIENCE DIRECT®
Aquatic Living Resources 16 (2003) 137–144
Aquatic Living Resources
www.elsevier.com/locate/aquliv

Three-dimensional acoustic mapping and simulation of krill distribution in the Saguenay—St. Lawrence Marine Park whale feeding ground

Yvan Simard [a,*], Denis Marcotte [b], Keyvan Naraghi [b]

[a] *Institut des Sciences de la Mer de Rimouski, Université du Québec à Rimouski, 310 Allée des Ursulines, Rimouski, Québec, Canada G5L 3A1, and Institut Maurice-Lamontagne, Pêches et Océans Canada, C.P. 1000, Mont-Joli, Québec, Canada G5H 3Z4*
[b] *Département des Génies Civil, Géologique et des Mines, École Polytechnique, C.P. Centre-ville, Montréal, Québec, Canada H3C 3A7*

Accepted 10 January 2003

Abstract

Geostatistical conditional simulations are used to get a family of non-smoothed three-dimensional (3D) images of the St. Lawrence krill aggregation from echointegration data at 38 and 120 kHz on a systematic grid of transects. These maps respect the inherent patchiness of krill. Their ensemble gives an histogram of the krill density estimates at any point of the 3D grid, not only the mean density as in kriging. The spatially consistent simulations are conditional to match the observations and their histogram and variogram. The 3D problem is by-passed by transposing to a short series of 2D ones, which simplifies the modelling of the autocorrelation function and has the additional advantage of reducing by a factor of 5 the number of points to simulate. The spatially structured krill density profile is summarised by the first few factors of a principal component analysis, where the variables are the volume backscattering strength at 120 kHz for the integrated vertical bins along the profiles and the observations are the different profiles. The principal component scores are simulated over a 2D-grid and then used to reconstruct the full 3D-image. The method adequately reproduces the histogram, variogram and mean profile of krill density, and cross-validations replicate the observations. It is as precise as an alternative kriging approach to estimate the mean density, but has the additional advantages of requiring less computing time for our particular application. These conditional simulations enable estimating the probability density function of the krill density at any point, an essential information for predator-prey interactions and other ecosystem studies.

Keywords: Acoustics; Conditional simulation; Geostatistics; St. Lawrence estuary; Whale feeding ground

1. Introduction

Oceans are three-dimensional (3D) spaces. Many properties measured in these ecosystems exhibit a structure over a range of scales in space and time (Haury et al., 1978; Mackas et al., 1985). Such structuring plays a fundamental role in ecosystem function from plankton (Steele, 1978) to whales (e.g. Simard et al., 2002). Vertical gradients tend to be several times larger than the horizontal ones. Oceans are also in motion and sampling effectively in time and space can be difficult. Acoustics tools can sample these huge 3D-environments remotely, rapidly and continuously. Acoustics has been used for seafloor mapping and, given sufficient time, a complete high-resolution image of the seabed on continental shelves can be obtained from multibeam sonar imaging. The equivalent for the moving pelagic environment and its drifting or actively mobile content is not possible, nor relevant. At best, acoustic imaging can produce a time-distorted tomography of the pelagic systems, via the assembly of a series of slices through the body of water (e.g. Greene et al., 1998; Stanley et al., 2000). Multibeam sonars can be used to get high-resolution series of slices in close range of a sampling vessel (e.g. Gerlotto et al., 1999). Though this is useful for increasing the information available at small scales, it only slightly enlarges the slice width when we consider the scale of the transects covered by the sampling vessel over what are often very large study areas. Furthermore, because the observation angle varies for each beam of the multibeam sonar, these observations must be interpreted with caution because of the strong directivity patterns of the backscattering from fish or zooplankton targets (Medwin and Clay, 1998). Low frequency sonars could help to enlarge the observation slice width up to kilometres for highly reflective large targets, but

* Corresponding author.
E-mail address: simardy@dfo-mpo.gc.ca (Y. Simard).

doi:10.1016/S0990-7440(03)00026-3

the sampled field then is still only a fraction of the water column, that depends on the propagation characteristics in the medium (Farmer et al., 1999).

To get a best estimate of the 3D-distribution of a resource in large pelagic ecosystems from limited survey transects, the 3D-image must be reconstructed from the series of comparable observation slices, ideally from the same vertical viewing angle because of the sound scattering directivity of the targets. This can be done by 3D-kriging (Chilès and Delfiner, 1999), taking advantage of the strong autocorrelation in acoustic data (e.g. Simard et al., 1993) to estimate the values at unvisited locations between the observed slices[1]. The required anisotropic 3D-variogram is, however, difficult to define with accuracy because it must take into account a gradient along the vertical axis that is very different from those along the horizontal axes in combination with krill patchiness. For example, krill scattering layers (SLs) can extend several tenths of kilometre horizontally, but start and stop abruptly at a scale of metre in the vertical (e.g. Lavoie et al., 2000). An alternative solution is to convert the 3D-problem to a 2D one, by summarising the vertical profiles of observations by a fitted function (e.g. Goulard and Voltz, 1993), and kriging its parameters. The function is then used with the estimated parameter to produce a mean estimate of the studied variable at each node of the series of nodes making the 3D-estimation grid. Since kriging is a smoother, this value does not represent the full range of values that could be observed at a node. This variability (i.e. patchiness) is, however, an important characteristic of the ecosystem, that must be taken into account to understand the interactions between predators and preys in 3D pelagic ecosystems (e.g. Zamon et al., 1996). Any feeding functional response is dependent on prey density. In optimising this function through their feeding strategies, predators must preferably look for the richest densities, not for the mean density. This is particularly true for whales, for which efficient feeding in the ocean is critical (e.g. Acevedo-Gutierrez et al., 2002). Conditional geostatistical simulations (Chilès and Delfiner, 1999) is a spatial approach that can take this relevant local prey density distribution into account, by producing a series of realisations of the grid estimates, from which a probability density function (pdf) of prey density can be computed for each node of the grid. Chilès and Delfiner (1999) define these methods as "spatially consistent Monte Carlo simulations". They produce realistic pictures of spatial variability by introducing an autocorrelated random component in the geostatistical estimation process, which is not done in kriging. Therefore, conditional simulations produce non-smoothed pictures of the reality contrary to kriging estimates. On an average, the same patchiness as that of the unknown reality is expected on the simulation.

In this paper, we apply a 2D-approach and conditional simulations to estimate multiple realisations of the 3D krill aggregation of the Saguenay—St. Lawrence Marine Park, from a series of acoustic echointegration slices. Several species of toothed and baleen whales frequent this traditional feeding ground in summer (Michaud et al., 1997). Understanding the local trophic interaction dynamics that is acting during research surveys requires realistic estimations of the prey fields available to these predators, whose success relies on large amounts of densely concentrated food. The method we adopted here is general and can be easily applied to several other studies, where a multivariate signal has to be generated over a continuous field from spatially structured sparse observations.

2. Material and methods

2.1. Sampling

Sampling was carried out aboard the Canadian Coast Guard Ship "*F.G. Creed*" in the St. Lawrence estuary on 31 July and 1 August 1994, along a regular grid of 10 transects crossing the head of the Laurentian channel (Fig. 1). Sampling procedures are briefly outlined here; details can be found in Simard and Lavoie (1999). The grid was surveyed during daytime only, when the krill SLs were at their daytime depth (Simard et al., 1986) and well separated from fish echoes in the upper water column. CTD profiles and zooplankton samples from 0.28-m^2 Bongo nets were taken at stations along the transects (Fig. 1). Acoustic backscattering coefficient (s_v) data at 120 kHz (3.3° beam) and 38 kHz (10° beam) were acquired from a Biosonics 102 echosounder linked to a computer via a Biosonics ESP A/D interface and the ESP_EI echointegration software, which simultaneously recorded positions from a GPS receiver. At the beginning of the survey, the ambient noise level at the survey speed was recorded for each frequency, with the transducers in listening mode (i.e. not transmitting). ESP_EI software was then set up to only accept echoes, whose voltage exceeded the measured noise level for each vertical stratum. Echointegration (MacLennan and Simmonds, 1992) was done along transects on 5-m vertical strata, from ranges of 2 to 207 m, which included all the krill SLs. Horizontally, echointegration was done every 20 pings (20 s), which corresponded to steps of ~80 m at the survey speed of 8 knots. The acoustic data used hereafter were, therefore, s_v profiles with a vertical resolution of 5 m and spaced every 80 m along transects. The system was calibrated using the standard sphere method for each frequency (Foote et al., 1987).

2.2. Data analysis

The acoustic backscattering coefficient data were cleaned of acoustic interference and the first meter off the bottom was ignored. They were corrected for the absorption (François and Garrison, 1982) and sound speed profile associated to the vertical structure of the water column. The resulting s_v at 120 kHz was used for the present krill biomass simulations,

[1] Introductions to geostatistical methods in fisheries applications can be found in Petitgas (1996) or Rivoirard et al. (2000).

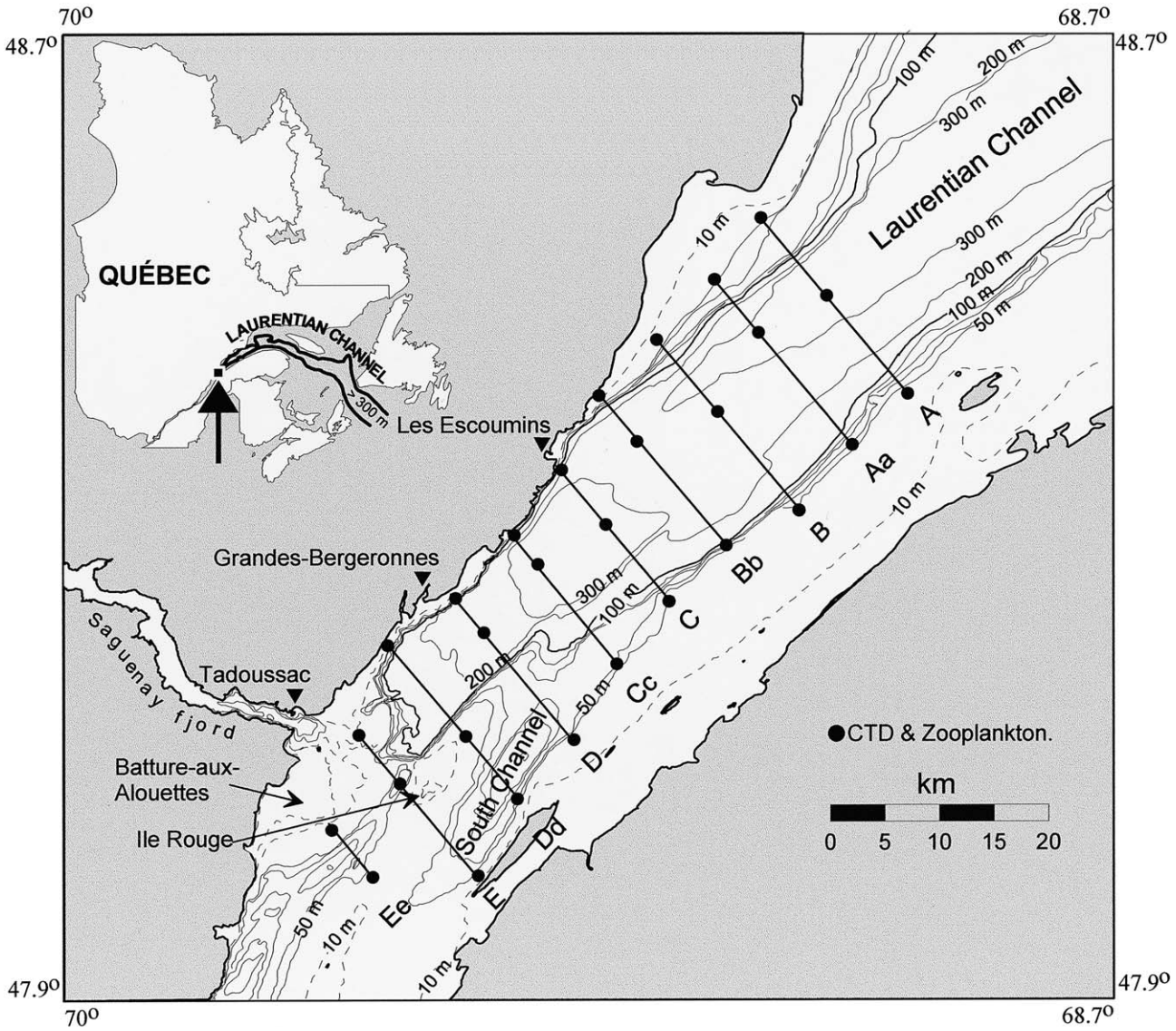

Fig. 1. Map of the study area showing the acoustic transects, and the hydrographic and plankton stations.

after the fish echoes were sorted out using the s_v ratio at the two frequencies (Simard and Lavoie, 1999). The acoustic densities were converted to biomass using a mean target strength of –69 dB g^{-1} (see Simard and Lavoie, 1999). The s_v profiles containing krill in more than 2 strata between the depth limits of the krill SL (ranges of 27–207 m) were used as the basis for the simulation (Fig. 2a, red). The simulation domain was limited to areas, where the bottom depths exceeded 50 m, the observed krill SLs being confined to deeper waters (Fig. 2a–c).

The simulation proceeded in four steps. First, the data were prepared for a principal component analysis (PCA, Lebart et al., 1984), whose output will be used for summarising the s_v profile shapes by a few orthogonal (i.e. uncorrelated) principal components (PCs). Each profile was represented by the 37 s_v values corresponding to the 5–m bin strata, where the krill SL was present. The zeros present on some profiles and the strata below the bottom depth were assigned an artificial small s_v value of 3.16×10^{-9} m^{-1} (or an equivalent volume backscattering strength, $S_v = 10 \log_{10}(s_v) = -85$ dB) to provide complete profiles of 37 values everywhere and to allow for a log transformation prior to the PCA analysis. This artificial s_v value was derived from a simulation study, where different candidate values were tested. The value was selected to ensure a non-biased mean s_v value computed from 100 realisations obtained following the same method as described below. The data were log-transformed to S_v to stabilise the variances, thus, giving a more stable PCA analysis than with the raw data.

Second, a PCA was performed on the centred S_v profiles to reduce the representation of their shapes from initially 37 variables (strata) to 7 orthogonal PCs. The number of significant PCs retained was determined by requiring a minimum of 85% of the total variance be accounted for, by

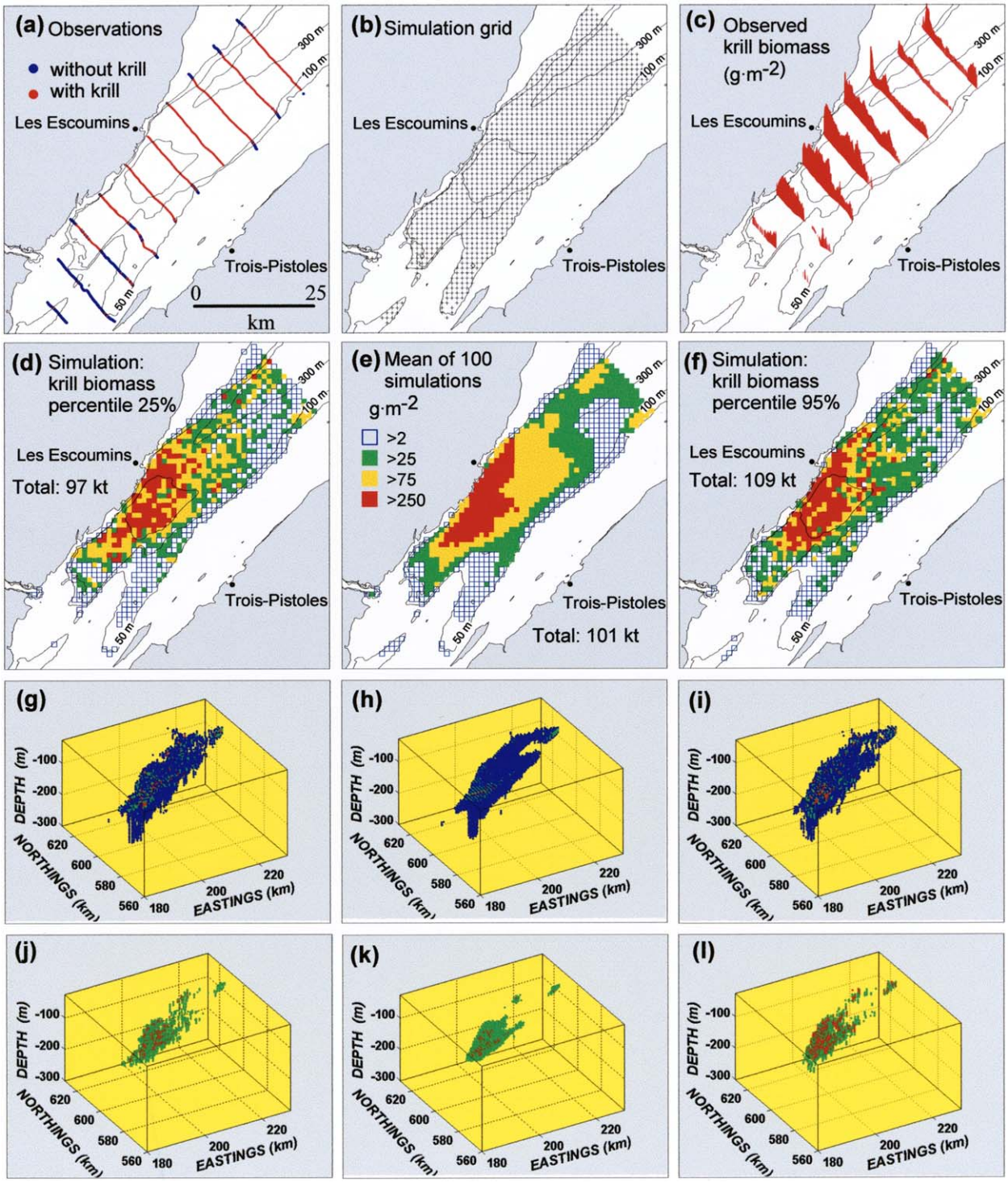

Fig. 2. Simulation of the krill aggregation. Location of the observed acoustic profiles with (red) and without (blue) krill (a), grid nodes used for simulating the S_v profiles (b), observed vertically integrated krill biomass with a square-root symbol height scale (c). Vertically integrated krill biomass maps for a simulation where the total biomass corresponded to the first quartile of cumulated density function of the total biomass of the 100 simulations (d), to the mean of the 100 simulations (e), and to the 95th percentile of the same cumulated density function of the total biomass (f). 3D view of the simulated biomass corresponding to d–f for the richest quartile (g–i) or the richest 5% (j–l) based on the krill concentration cut-offs from the mean of the 100 simulations; the three-colour palette cut-offs being blue, >0.6 gm^{-3}; green, >3.7 gm^{-3}; red, >8.1 gm^{-3}.

examination of the eigenvalues plot searching for a clear break in the slope, and by retaining only the PC scores with the nugget component on the experimental variograms smaller than half the sill.

Third, the scores on the retained PCs were graphically gaussian-transformed (required for the simulation method below) and subjected to geostatistical conditional simulations (Chilès and Delfiner, 1999). Each gaussian-transformed

Table 1
Percentage of variance explained by the first seven PCs and parameters of the anisotropic spherical model [a] fitted to the variograms of the observed PC scores. Directions are geometric degrees, 45° being the channel axis. C_0 is the nugget parameter

PC	% Variance	Direction 1	Dir. 2	a_1	a_2	C_0	C	C/C_0
1	52.5	45°	135°	38.00	14.80	0.154	0.898	5.83
2	11.7	45°	135°	38.00	13.70	0.167	1.288	7.71
3	10.0	45°	135°	12.36	19.96	0.364	0.727	2.00
4	5.7	45°	135°	8.77	7.40	0.320	0.710	2.22
5	3.5	45°	135°	14.80	5.96	0.407	0.639	1.57
6	2.3	45°	135°	7.34	4.40	0.474	0.522	1.10
7	1.7	45°	135°	11.10	5.10	0.451	0.597	1.32

[a] Model: $\gamma(h) = C_0 + \begin{cases} C\left(\frac{3h}{2a} - \frac{1}{2}\left(\frac{h}{a}\right)^3\right), & \text{if } h \leqslant a \\ C, & \text{if } h \geqslant a \end{cases}$

where h is the distance between the observations.

PC score was simulated separately using the covariance matrix decomposition (i.e. LU) method (Cholesky decomposition; Chilès and Delfiner, 1999). The covariance matrix, C, containing the covariances from the vector of the M conditional observation points plus the N points to simulate, is decomposed in a lower triangular matrix L so that $LL' = C$. The matrix L can be partitioned into four different blocks:

$$L = \begin{bmatrix} L_{MM} & 0 \\ L_{NM} & L_{NN} \end{bmatrix} \quad (1)$$

where L_{MM} corresponds to the set of conditioning points, L_{NN} to the set of points to simulate, and L_{NM} to the interaction between the two sets. A vector U, composed of $M + N$ independent $N(0,1)$ variables, completes the linear equation system:

$$\begin{bmatrix} Z_M \\ Z_n \end{bmatrix} = \begin{bmatrix} L_{MM} & 0 \\ L_{NM} & L_{NN} \end{bmatrix} \begin{bmatrix} U_M \\ U_N \end{bmatrix}$$

where Z_M is the conditional data and Z_N is the simulated data. The solution is:

$$\begin{aligned} Z_M &= L_{MM}\, U_M \\ U_M &= L_{MM}^{-1}\, Z_M \\ Z_N &= L_{NM}\, U_M + L_{NN}\, U_N \end{aligned} \quad (2)$$

One advantage of this LU decomposition method is that for computing another realisation of the simulation set Z_N, only the vector U_N of Eq. (2) has to be updated, which allows to realise several simulations without much additional computing cost. The simulation 1-km mesh grid (Fig. 2b) contained 1015 nodes where the bottom depth exceeded 50 m.

Fourth, the simulated gaussian-transformed PCA scores were back-transformed and then used, with the eigenvectors, to reconstruct the centred S_v profiles (Lebart et al., 1984). To insure that the histograms of the simulated and observed S_v are the same, a graphical transform (Chilès and Delfiner, 1999) mapping the simulated cumulative density function (cdf) to the observed cdf was applied.

An alternative to the above procedure, consisting of feeding the PCA with profiles that are limited to the water column and summarised by an equal number of points corresponding to relative (and not absolute) depths, was also tested. Local centring and standardisation of each profile combined with kriging of the mean and the variance in the final step was also explored, but did not performed better than the above global approach.

The accuracy of the method was tested through the following validation tests. First, we checked if the simulation reproduced the main descriptive statistics, the variogram, and the pdf of the observed data. Second, a cross validation at small distances was performed by removing one S_v profile every two profiles and simulating the removed profiles using the remaining profiles as conditional data. Third, the performance at larger distances was checked by randomly picking up 100 conditional observations from a selection of one transect every two transects in the study area and simulating the profiles at 400 randomly chosen observations on the unselected alternating transects. Actual simulation conditions were less severe than those used for this test, the interpolation distances being at most half those of this test. Fourth, the means of the simulated data at the nodes of the 3D grid were also compared to those of a kriging using the same conditional data and the variogram computed for the first PC.

3. Results

The first seven PCs explained 87% of the variance of the S_v profiles (Table 1) and were retained for the simulation. The structural component (C,Table 1) of the corresponding PC scores was always larger than the unresolved variability (C_0,Table 1), up to more than five times for the first two PCs. The simulations closely reproduced the mean and the other distribution statistics of the observations (Table 2). The variograms of the simulated S_v were generally similar to the corresponding S_v, notably for the main krill concentration depth of about 80 m (Fig. 3). The small-distance cross validation showed that the simulations performed almost as well

Table 2
Descriptive statistics of the observed and simulated mean volume backscattering strength (S_v) of the profiles. Computed as acoustic backscattering coefficients (S_v), for each simulation, then averaged and transformed to s_v

Data	*n*	Mean	First quartile	Median	Third quartile	Max
Observed	1368	–70.2	–77.4	–72.8	–68.5	–59.4
Simulated	1015	–71.0	–78.6	–74.8	–69.6	–61.8

as kriging to replicate the observations (Fig. 4a,b). Results of the two approaches of cross validation at large distances were nearly identical (Fig. 4c,d). The 2D-map of the krill biomass obtained from the mean of all simulations (Fig. 2e) was almost identical to that computed by Lavoie et al. (2000, Fig. 9d) from a 2D-kriging. Its total integrated biomass of 101 kt fell within the 95% confidence interval of Simard and Lavoie's (1999) kriging estimate for this survey. The individual simulation having a total biomass equal to that of the first quartile of the total biomass cdf of all simulations (Fig. 2d) presented much more "grain" or patchiness than that of the mean, as expected. The same was true for the simulation corresponding to the 95th percentile of the same cdf (Fig. 2f). This enhanced patchiness of the individual simulations compared to the mean of all simulations (or kriging results not shown) was also evident in 3D (Fig. 2g–l).

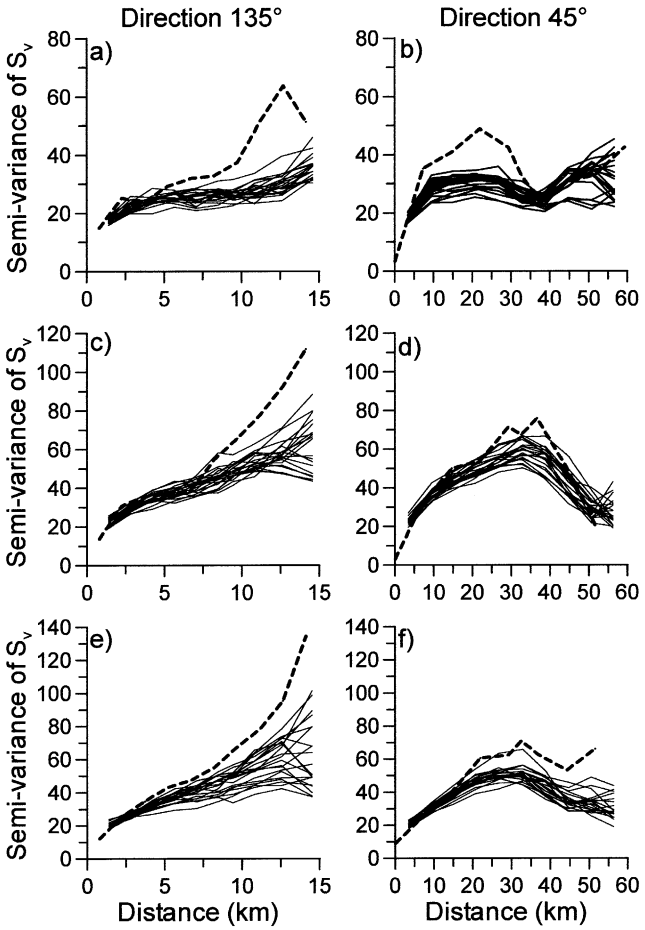

Fig. 3. Comparisons of variograms of simulated S_v for 20 randomly selected simulations (thin lines) with the variograms of observed S_v (bold line) in the transect direction (135°) and along channel (45°) for three depths: 59.5 m (a, b), 79.5 m (c, d), and 99.5 m (e, f).

The mean simulated biomass profile had the same amplitude, envelope and modal depth than the observed one (Fig. 5).

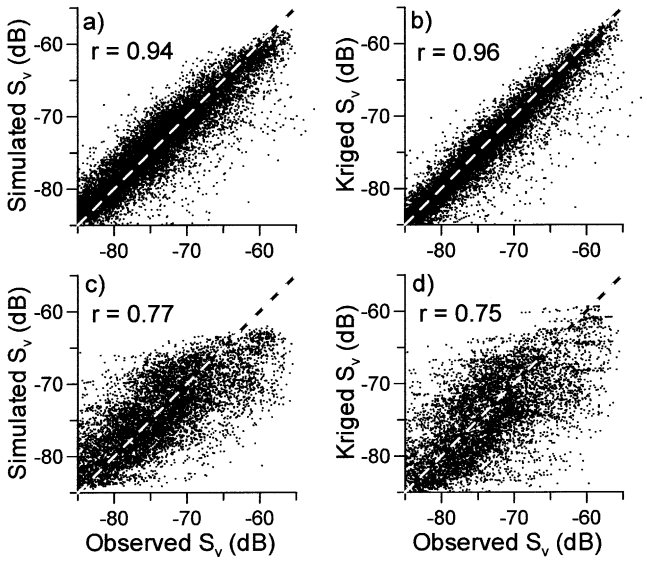

Fig. 4. Comparison between kriged estimates and the mean of 100 simulations with the observations for short distances (along transects) (a, b) and longer distances (to the next transect) (c, d). Lines are $y = x$.

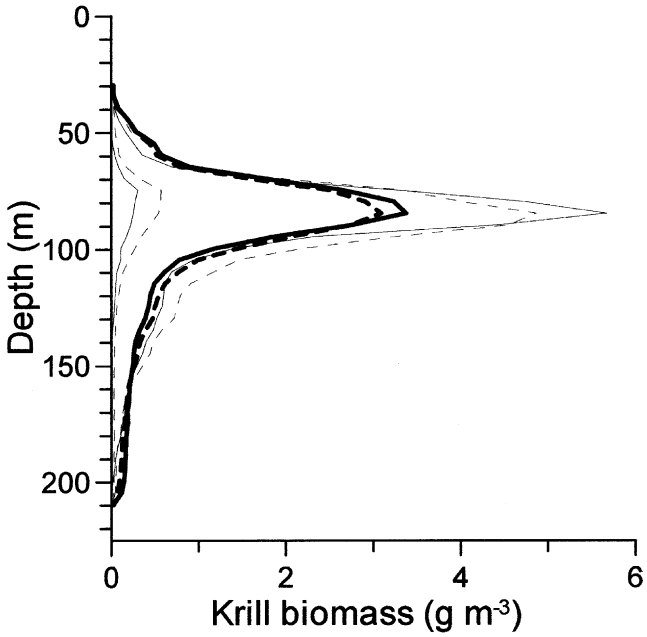

Fig. 5. Comparison of observed (continuous lines) and simulated (dashed lines) krill biomass profiles. Means (bold lines), first and third quartiles (thin lines).

4. Discussion

The proposed 2D approach to solve the difficulty of geostatistically mapping a structured variable in 3D appears to perform relatively well with krill acoustic densities collected along line transects. Coupled with conditional simulations, this approach becomes an efficient way of exploring the space of variability of 3D-structured data, such as the S_v at several acoustic frequencies, or exploitations of such information to generate secondary variables, including taxonomic composition or acoustical description of the bottom. The interest of having a series of realistic simulations instead of only a mean estimate allows for much more possibilities of using the information for better interpretation of the results. For example, 3D-maps of the probability to exceed the given krill density thresholds, an important variable for predator/prey interactions, can be obtained directly from the simulated data. The fraction of the total biomass above this threshold (e.g. exploitable biomass) is another information directly available. Simulations also allow to see realistic pictures of krill patchiness, the distribution of the rich nuggets that predators could detect and exploit, which are totally invisible to alternative smoothing methods. The exploitation of such methods appears, therefore, very useful for helping to understand the actual functioning of our 3D-structured ocean ecosystems.

Though the numerical methods are relatively simple, their applications to actual observed data ask for particular attributes of the data set and require some data conditioning to satisfy the numerical conditions. First, the zero profiles pose problems in defining the simulation field. In our case, the krill aggregation was a continuous cloud and the zero profiles were located at its periphery. It was then simple to limit the simulation grid to the contour of the aggregation. If this had not been the case, the simulation grid nodes would have been to be determined first, from 2D indicator conditional simulations (Chilès and Delfiner, 1999) of the null node locations. Second, the zero part of the profiles and the empty cells below the seafloor need to be filled for performing the PCA. A possible practical solution is to use a relative vertical scale, such as the proportion of the water column, instead of the absolute depth. Though this solution was initially tried, we preferred to work in absolute units because krill are vertically distributed along the depth. This structure is distorted by relative units. Instead, we chose to fill the empty cells of the profiles by a non-biasing low s_v value. This step is the most demanding in terms of computing time. An alternative approach would be to use a transformation that could handle zeros more easily than the log one (e.g. square root, cubic root, Box-transform). Third, the PCs must be spatially uncorrelated among them for all lag distances, not only for zero lag as PCA provides by construction. This is especially important for small distances, such as half the transect spacing. Cross-correlations at larger distance have less impact because the conditioning observations are imposing the larger scale spatial structure, a characteristic of conditional simulations. We checked if the main PCs were cross-correlated over small lag distances and found only low correlations ($r < |0.25|$), often linearly sloping around zero. Our implicit assumption of negligible cross-correlation of PCs was therefore reasonable. Fourth, LU decomposition method of the covariance matrix is limited to small matrices. The size of our data set was at about the limit for this method. For larger data sets (or lower level computers) a solution to this problem, is to partition the study area into adjacent small neighbourhoods and perform the simulation in a sliding window. To prevent the creation of artificial discontinuities between the neighbourhoods, the conditional data for the neighbourhoods can include the simulated data of the preceding neighbourhood (Alabert, 1987). Also, several simulation methods are able to handle large grids (e.g. turning bands, SGS, FFT-MA, etc.; see Chilès and Delfiner, 1999).

References

Acevedo-Gutierrez, A., Croll, D., Thershy, B., 2002. Feeding costs limit dive time in large whales. J. Exp. Mar. Biol. 205, 1747–1753.

Alabert, F., 1987. The practice of fast conditional simulations through the LU decomposition of the covariance matrix. Math. Geol. 19, 369–386.

Chilès, J.-P., Delfiner, P., 1999. Geostatistics: Modeling Spatial Uncertainty. John Wiley and Sons, Inc., New York.

Farmer, D.M., Trevorrow, M.V., Pedersen, B., 1999. Intermediate range fish detection with a 12–kHz sidescan sonar. J. Acoust. Soc. Am. 106, 2481–2490.

Foote, K.G., Knudsen, H.P., Vestnes, G., MacLennan, D.N., Simmonds, E.J., 1987. Calibration of acoustic instruments for fish density estimation: a practical guide. ICES Coop. Res. Rep. No. 144 .

François, R.E., Garrison, G.R., 1982. Sound absorption based on ocean measurements: Part II: Boric acid contribution and equation for total absorption. J. Acoust. Soc. Am. 72, 1879–1890.

Gerlotto, F., Soria, M., Fréon, P., 1999. From two dimensions to three: the use of multibeam sonar for a new approach in fisheries acoustics. Can. J. Fish. Aquat. Sci. 56, 6–12.

Goulard, M., Voltz, M., 1993. Geostatistical interpolation of curves: a case study in soil science. In: Soares, A (Ed.), Geostatistics Troia '92, vol. 2. Kluwer Academic Publisher, Dordrecht, pp. 805–816.

Greene, C.H., Wiebe, P.H., Pelkie, C., Benfield, M.C., Popp, J.M., 1998. Three-dimensional acoustic visualization of zooplankton patchiness. Deep-Sea Res. II. 45, 1201–1217.

Haury, L.R., McGowan, J.A., Wiebe, P.H., 1978. Patterns and processes in the time-space scales of plankton distributions. In: Steele, J.H (Ed.), Spatial Pattern in Plankton Communities. Plenum Press, New York, pp. 277–327.

Lavoie, D., Simard, Y., Saucier, F.J., 2000. Aggregation and dispersion of krill at channel heads and shelf edges: the dynamics in the Saguenay—St. Lawrence Marine Park. Can. J. Fish. Aquat. Sci. 57, 1853–1869.

Lebart, L., Morineau, A., Warwick, K.M., 1984. Multivariate Descriptive Statistical Analysis: Correspondence Analysis and Related Techniques for Large Matrices. John Wiley and Sons, New York.

Mackas, D.L., Denman, K.L., Abbott, M.R., 1985. Plankton patchiness: biology in the physical vernacular. Bull. Mar. Sci. 37, 652–674.

MacLennan, D.N., Simmonds, E.J., 1992. Fisheries Acoustics. Chapman and Hall, London.

Medwin, H., Clay, C.S., 1998. Fundamentals of Acoustical Oceanography. Academic Press, New York.

Michaud, R., Bédard, C., Mingelbier, M., Gilbert, M.C., 1997. Les activités d'observation en mer des cétacés dans l'estuaire maritime du Saint-Laurent 1985–1996 : une étude de la répartition spatiale des activités et des facteurs favorisant la concentration des bateaux sur les sites d'observation. GREMM, 108 de la Cale Sèche, Tadoussac, Québec G0T 2A0. Final report to Parks Canada, Canadian Heritage Department, Ottawa 17 p.

Petitgas, P., 1996. Geostatistics and their applications to fisheries survey data. In: Megrey, B.A., Mokness, E (Eds.), Computers in Fisheries Research. Chapman and Hall, UK, London, pp. 113–142.

Rivoirard, J., Simmonds, J., Foote, K.G., Fernandes, P., Bez, N., 2000. Geostatistics for Estimating Fish Abundance. Blackwell Science, Oxford.

Simard, Y., Lacroix, G., Legendre, L., 1986. Diel vertical migrations and nocturnal feeding of a dense coastal krill scattering layer (*Thysanoessa raschi* and *Meganyctiphanes norvegica*) in stratified surface waters. Mar. Biol. 91, 93–105.

Simard, Y., Lavoie, D., 1999. The rich krill aggregation of the Saguenay—St. Lawrence Marine Park: hydroacoustic and geostatistical biomass estimates, structure, variability and significance for whales. Can. J. Fish. Aquat. Sci. 56, 1182–1197.

Simard, Y., Lavoie, D., Saucier, F.J., 2002. Channel head dynamics: Capelin (*Mallotus villosus*) aggregation in the tidally-driven upwelling system of the Saguenay—St. Lawrence Marine Park's whale feeding ground. Can. J. Fish. Aquat. Sci. 59, 197–210.

Simard, Y., Marcotte, D., Bourgault, G., 1993. Exploration of geostatistical methods for mapping and estimating acoustic biomass of pelagic fish in the Gulf of St. Lawrence: size of echointegration unit and auxiliary environmental variables. Aquat. Living Resour. 6, 185–199.

Stanley, R.D., Kieser, R., Cooke, K., Surry, A.M., Mose, B., 2000. Estimation of a widow rockfish (*Sebastes entomelas*) shoal off British Columbia, Canada as a joint exercise between stock assessment staff and the fishing industry. ICES J. Mar. Sci. 57, 1035–1049.

Steele, J.H., 1978. Spatial Pattern in Plankton Communities. Plenum Press, New York.

Zamon, J.E., Greene, C.H., Meir, E., Demer, D.A., Hewitt, R.P., Sexton, S., 1996. Acoustic characterization of the three-dimensional prey field of foraging chinstrap penguins. Mar. Ecol. Prog. Ser. 131, 1–10.